Magnetization Factors of Gamma-Ray Burst Jets Revealed by a Systematic Analysis of the Fermi Sample

An Li, He Gao, Lin Lan, Bing Zhang (ApJ, September 1, 2024)

Reporter: Dan Zhu

Date: 2025/5/9

1.Introduction

- Gamma-ray bursts (GRBs) are among the most energetic events in the universe.

- Central question: What is the composition of GRB jets?

  - Matter-dominated jets: It is assumed that the GRB outflows originate from an initially hot "fireball" composed of photons, electron/positron pairs and a small amount of baryons.

  - For GRBs that exhibit pure nonthermal spectra, the fireball model is challenged. It has been proposed that the GRB outflows should contain certain proportion of magnetic energy so that the contribution of the thermal component can be significantly reduced.

1. Introduction

Define the magnetization parameter： $\sigma_0 \equiv \frac{L_{c,0}}{L_{h,0}}$ ($L_{h,0}$: hot components luminosity; $L_{c,0}$: cold (Poynting flux) components luminosity).

In a hybrid jet scenario (Gao & Zhang 2015):

- $\sigma_0 \ll 1$: The spectrum is dominated by thermal components.
- Moderate values of σ_0: The thermal component becomes subdominant.
- Extremely large values of σ_0: Nonthermal radiation dominates (the thermal component is completely suppressed).

➢ Goal: measure σ_0 for a large Fermi GRB sample.

2. Data Reduction and Sample Selection

Fermi/GBM data selection criteria:

- Known redshift
- The signal-to-noise ratio (SNR) > 30

Sample: 87 GRBs divided into 318 time slices.

Spectral Fitting: Three models compared:

- Nonthermal (CPL/Band function)
- Hybrid (nonthermal + blackbody)
- Thermal (multicolor blackbody)

Model Selection: Bayesian Information Criterion (BIC). $\mathrm{BIC} = -2\ln L + k\ln(n)$

2. Data Reduction and Sample Selection

- **CPL model:** $F(E) = Ae^{-(2+\alpha)E/E_{\rm peak}}(\frac{E}{100\ \rm keV})^{\alpha}$,

- **Band model:**

$$F(E) = \begin{cases} A(\frac{E}{100\ \rm keV})^{\alpha} e^{-(2+\alpha)E/E_{\rm peak}}, & \text{if } E < \frac{(\alpha-\beta)E_{\rm peak}}{2+\alpha} \\ A(\frac{(\alpha-\beta)E_{\rm peak}}{(2+\alpha)100\ \rm keV})^{\alpha-\beta} e^{\beta-\alpha} (\frac{E}{100\ \rm keV})^{\beta}, & \text{otherwise} \end{cases}$$

where α and β are low-energy and high-energy photon spectral indices, respectively. E_{peak} is the υf_{υ} peak in keV.

- **Blackbody model:** $F(E) = A\frac{E^2}{e^{E/kT}-1}$, where kT is the temperature in unit of keV.

- **Multicolour blackbody model:**

$$N(E) = \frac{8.0525(m+1)K}{(\frac{T_{\rm max}}{T_{\rm min}})^{m+1}-1}(\frac{kT_{\rm min}}{\rm keV})^{-2} I(E)$$

$$I(E) = (\frac{E}{kT_{\rm min}})^{m-1} \int_{\frac{E}{kT_{\rm min}}}^{\frac{E}{kT_{\rm max}}} \frac{x^{2-m}}{e^x-1} dx$$

, where m is the power-law index of the Planck functions' distribution.

Statistical results:

Type	Number of Slices	GRB Quantity
nonthermal spectrum	225 slices	55
hybrid spectrum	81 slices	30
multicolour blackbody spectrum	12 slices	2

3. σ_0 Estimation

- **Key Parameters of GRB Jets:**

  - $\boldsymbol{r_0}$: The initial radius at which the jet emanates from the central engine.
  - $\boldsymbol{L_{\omega,0}}$: The total luminosity of the jet.
  - $\boldsymbol{\eta}$: The dimensionless entropy, defines average total energy (rest-mass energy + thermal energy) per baryon in the hot component.
  - $\boldsymbol{\sigma_0}$: The magnetization parameter at the central engine.

- **Jet Expansion and Acceleration**

  - After leaving the central engine, the jet will continuously expand and accelerate under the combined effects of thermal pressure and magnetic pressure until it reaches its maximum velocity $\Gamma_c \simeq \eta(1+\sigma_0)$ at the coasting radius r_c.
  - After the jet exceeds the photosphere radius r_{ph}, the photon optical depth for Thomson scattering drops below unity so that photons previously trapped in the jet can escape.

➢ Parameter Space and Analytical Model (Gao & Zhang, 2015)

- Divided the parameter space based on η and σ_0 and the relationship between r_{ph} and r_c into 4 regimes:

Table 2
Nondissipation Regime Criteria

Regime	Criteria
Regime II	$14.8(1+z)^{1/4}\left(\frac{kT_{\rm ob}}{50\ {\rm keV}}\right)^{1/4}\left(\frac{F_{\rm BB}}{10^{-8}\ {\rm erg\ s^{-1}cm^{-2}}}\right)^{3/16} r_{0,9}^{1/8} f_{\rm th,-1}^{1/2} f_{\gamma}^{1/2} d_{L,28}^{3/8} > 1$
$\eta > (1+\sigma_0)^{1/2}$	$0.24(1+z)^{-3}\left(\frac{kT_{\rm ob}}{50\ {\rm keV}}\right)^{-3}\left(\frac{F_{\rm BB}}{10^{-8}\ {\rm ergs^{-1}cm^{-2}}}\right)^{3/4} r_{0,9}^{-3/2} d_{L,28}^{3/2} > 1$
$r_{\rm c} > r_{\rm ph} > r_{\rm ra}$	$1.43 \times 10^{-5}(1+z)^{-7}\left(\frac{kT_{\rm ob}}{50\ {\rm keV}}\right)^{-7}\left(\frac{F_{\rm BB}}{10^{-8}\ {\rm ergs^{-1}cm^{-2}}}\right)^{7/4} r_{0,9}^{-7/2} f_{\rm th,-1}^{3} f_{\gamma}^{3} d_{L,28}^{7/2} < 1$
Regime III	$8.28(1+z)^{-3/2}\left(\frac{kT_{\rm ob}}{30\ {\rm keV}}\right)^{-3/2}\left(\frac{F_{\rm BB}}{10^{-7}\ {\rm ergs^{-1}cm^{-2}}}\right)^{5/8} r_{0,9}^{-1} f_{\rm th,-1}^{5/4} f_{\gamma}^{5/4} d_{L,28}^{5/4} > 1$
$\eta > (1+\sigma_0)^{1/2}$	$9.42 \times 10^{-2}(1+z)^{-14/3}\left(\frac{kT_{\rm ob}}{30\ {\rm keV}}\right)^{-14/3}\left(\frac{F_{\rm BB}}{10^{-7}\ {\rm ergs^{-1}cm^{-2}}}\right)^{7/6} r_{0,9}^{-7/3} f_{\rm th,-1}^{2} f_{\gamma}^{2} d_{L,28}^{7/3} > 1$
$r_{\rm ph} > r_{\rm c}$	
Regime V	$41.4(1+z)^{1/2}\left(\frac{kT_{\rm ob}}{10\ {\rm keV}}\right)^{1/2}\left(\frac{F_{\rm BB}}{10^{-9}\ {\rm ergs^{-1}cm^{-2}}}\right)^{3/8} r_{0,9}^{-1/4} f_{\rm th,-1} f_{\gamma} d_{L,28}^{3/4} < 1$
$\eta < (1+\sigma_0)^{1/2}$	$5.28(1+z)^{-3}\left(\frac{kT_{\rm ob}}{10\ {\rm keV}}\right)^{-3}\left(\frac{F_{\rm BB}}{10^{-9}\ {\rm ergs^{-1}cm^{-2}}}\right)^{3/4} r_{0,9}^{-3/2} d_{L,28}^{3/2} > 1$
$r_{\rm c} > r_{\rm ph} > r_{\rm ra}$	$1.16 \times 10^{-5}(1+z)^{-8}\left(\frac{kT_{\rm ob}}{10\ {\rm keV}}\right)^{-8}\left(\frac{F_{\rm BB}}{10^{-9}\ {\rm erg\ s^{-1}cm^{-2}}}\right) r_{0,9}^{-3} f_{\rm th,-1} f_{\gamma} d_{L,28}^{2} < 1$
Regime VI	$8.28(1+z)^{-3/2}\left(\frac{kT_{\rm ob}}{30\ {\rm keV}}\right)^{-3/2}\left(\frac{F_{\rm BB}}{10^{-7}\ {\rm ergs^{-1}cm^{-2}}}\right)^{5/8} r_{0,9}^{-1} f_{\rm th,-1}^{5/4} f_{\gamma}^{5/4} d_{L,28}^{5/4} < 1$
$\eta < (1+\sigma_0)^{1/2}$	$5.63 \times 10^{-3}(1+z)^{-8/3}\left(\frac{kT_{\rm ob}}{30\ {\rm keV}}\right)^{-8/3}\left(\frac{F_{\rm BB}}{10^{-7}\ {\rm ergs^{-1}cm^{-2}}}\right)^{1/3} r_{0,9}^{-1} f_{\rm th,-1}^{1/3} f_{\gamma}^{1/3} d_{L,28}^{2/3} > 1$
$r_{\rm ph} > r_{\rm c}$	

➢ Parameter Space and Analytical Model (Gao & Zhang, 2015)

- For each regime, an analytical model connects GRB spectrum observables with central engine parameters:

$$1+\sigma_0 = \begin{cases} 25.5(1+z)^{4/3}(\frac{kT_{\rm ob}}{50{\rm keV}})^{4/3}(\frac{F_{\rm BB}}{10^{-8}{\rm erg\ s^{-1}cm^{-2}}})^{-1/3} r_{0,9}^{2/3} f_{\rm th,-1}^{-1} f_\gamma^{-1} d_{\rm L,28}^{-2/3}, & \text{Regime I} \\ 5.99(1+z)^{4/3}(\frac{kT_{\rm ob}}{30{\rm keV}})^{4/3}(\frac{F_{\rm BB}}{10^{-7}{\rm erg\ s^{-1}cm^{-2}}})^{-1/3} r_{0,9}^{2/3} f_{\rm th,-1}^{-1} f_\gamma^{-1} d_{\rm L,28}^{-2/3}, & \text{Regime II and III} \\ 6.43(1+z)^{4/3}(\frac{kT_{\rm ob}}{10{\rm keV}})^{4/3}(\frac{F_{\rm BB}}{10^{-9}{\rm erg\ s^{-1}cm^{-2}}})^{-1/3} r_{0,9}^{2/3} f_{\rm th,-1}^{-1} f_\gamma^{-1} d_{\rm L,28}^{-2/3}, & \text{Regime IV} \end{cases}$$

Where $f_{th} = F_{BB}/F_{ob}$, $f_\gamma = L_\gamma/L_\omega$, $L_\omega = 4\pi d_L^2 F_{ob}/f_\gamma$, T_{ob} is the observed blackbody temperature, L_ω is the wind luminosity, F_{BB} is the observed blackbody flux, F_{ob} is the observed total flux (both thermal and nonthermal included), d_L is the luminosity distance. Fix: f_γ =0.5; r_0: $10^8 cm, 10^9 cm, 10^{10} cm$.

➢ The estimated σ_0 for the three spectral types:

- Thermal-dominant spectra: In the case of 12 slices with thermal-dominant spectra, we set their σ_0 equal to 0.

- Hybrid spectra: We have 81 slices with hybrid spectra, for which we calculated their σ_0 values based on the extracted quantities such as T_{ob}, F_{BB} and f_{th} by fitting the spectrum.

- Nonthermal spectra: We have 225 slices with nonthermal spectra, for which we estimate the lower limit of their σ_0 value by simulating the upper limit of the thermal component.

4. result

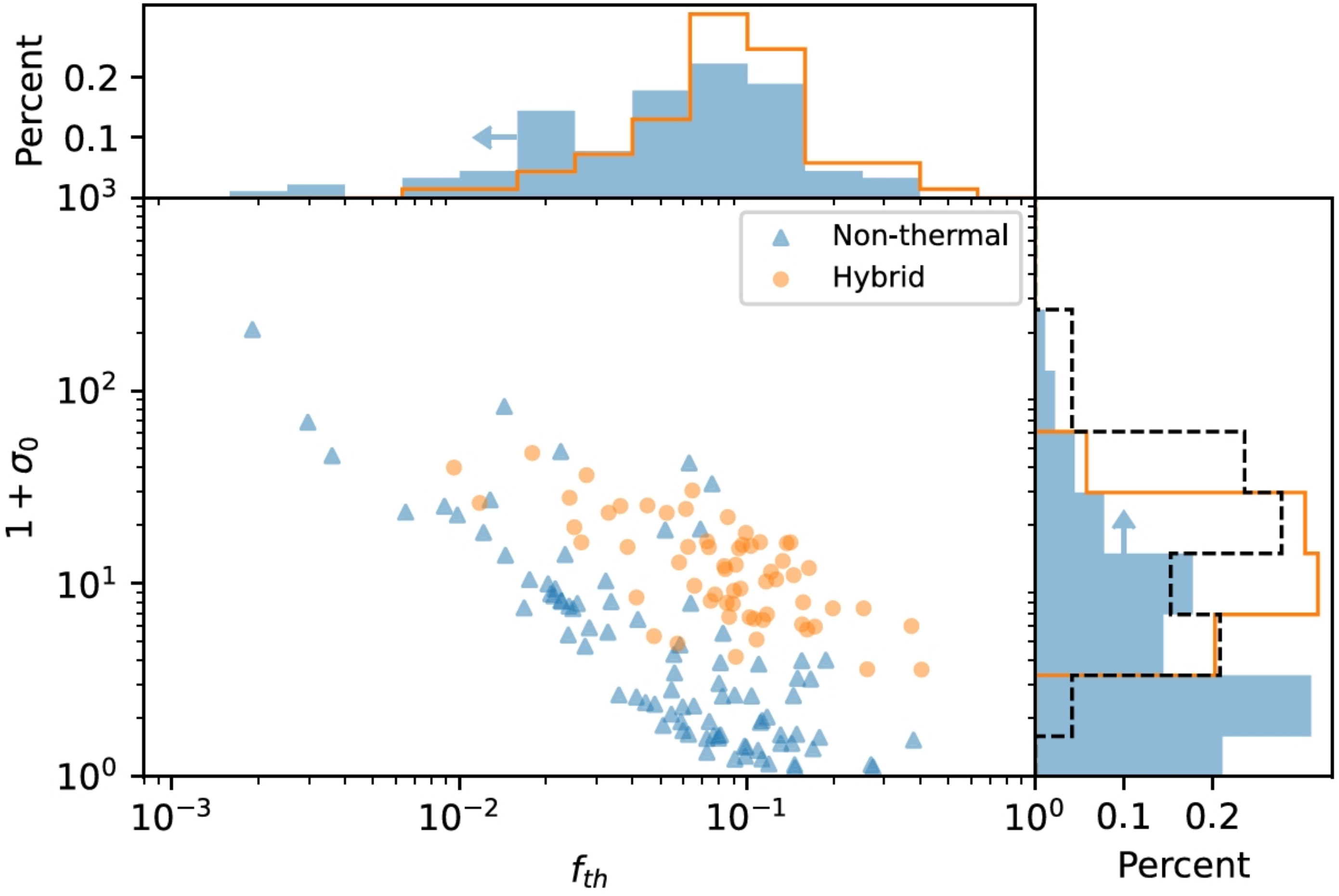

Figure1. Distribution plot of $1+\sigma_0$ and f_{th}.

- Hybrid spectrum: $1+\sigma_0$ ranges from 3.6-47.7 (peak at 11.9); f_{th} ranges from 0.009-0.4 (peak at 0.08).

- Nonthermal spectrum: $1+\sigma_0$ ranges from 1.1-424.9 (with ~23% larger than 10); f_{th} ranges from 0.003-0.4.

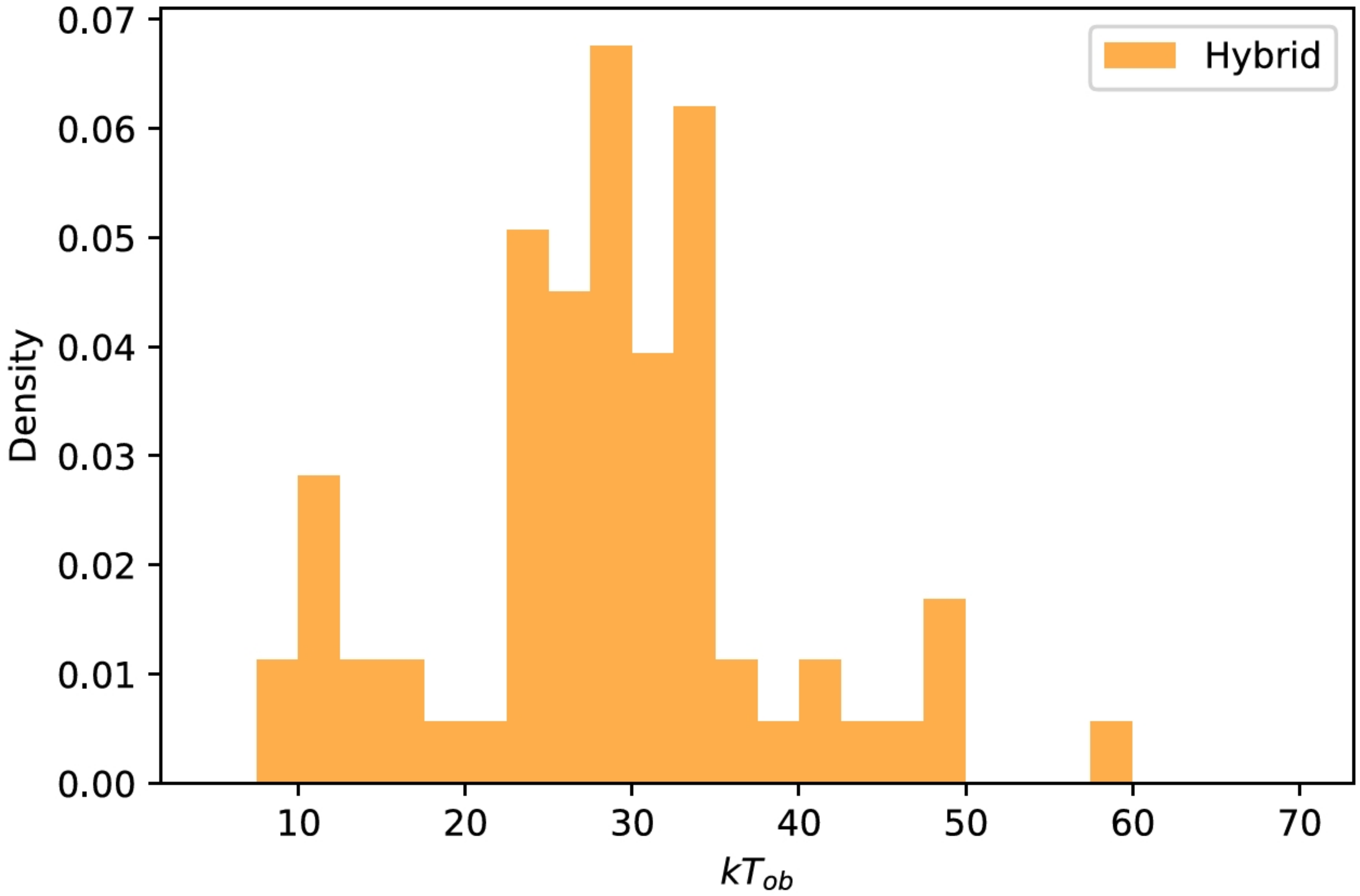

Figure 2. The distribution of KT_{ob} in the GRB with hybrid spectrum.

Hybrid spectrum: the values of KT_{ob} are distributed in the range of 8.5–58.7 keV, with the average value located at 28.4 keV with a variance of 10.5 keV.

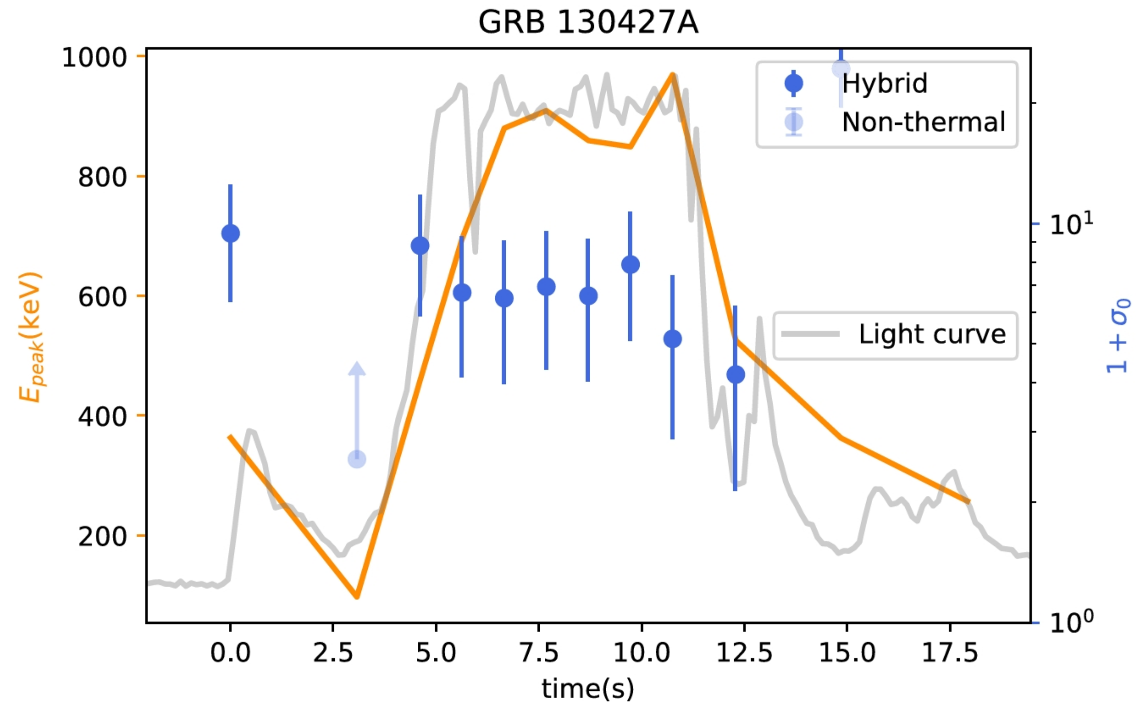

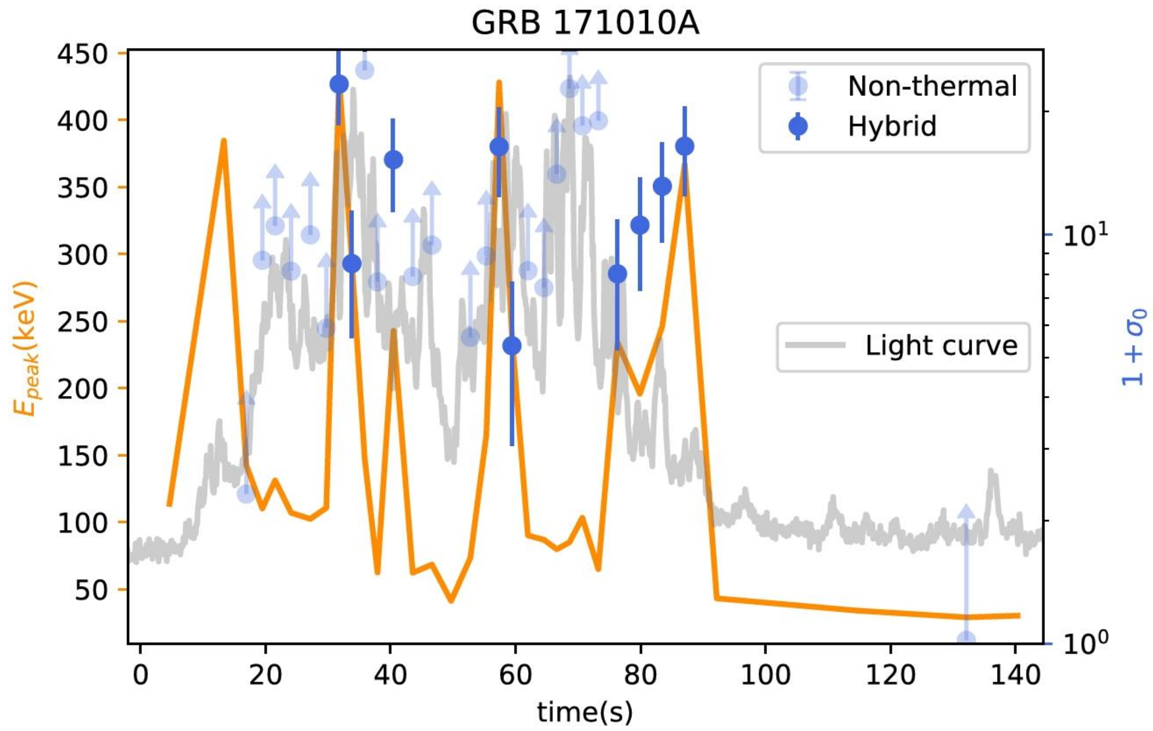

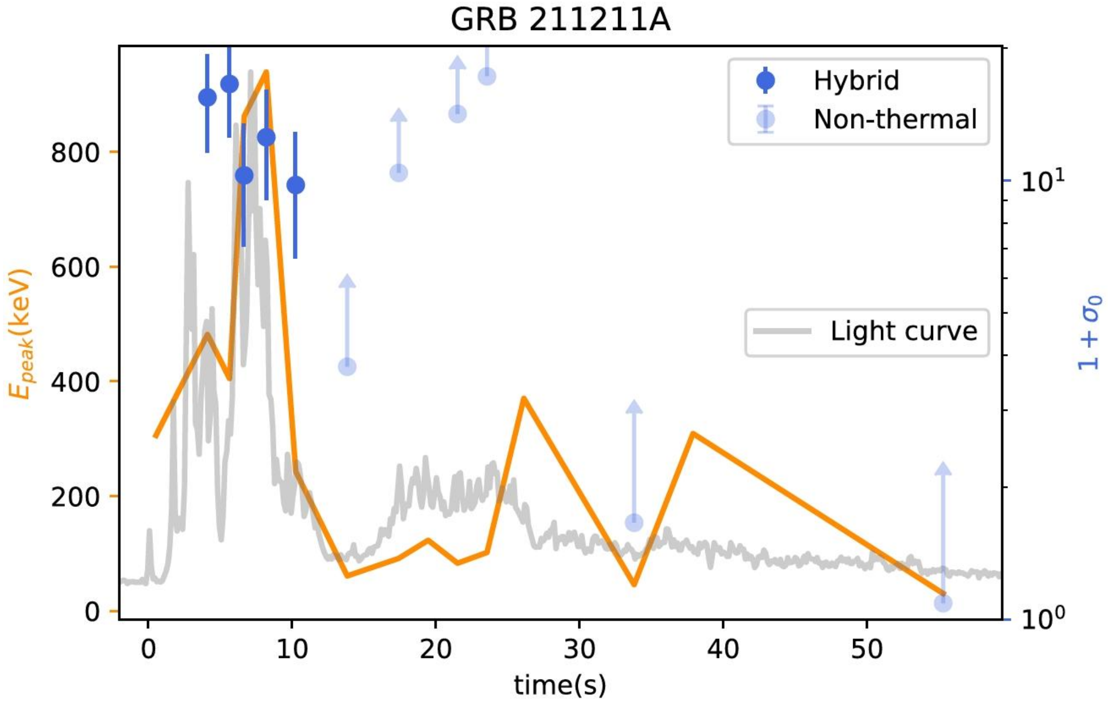

Figure3. Evolution of photon counts, $1+\sigma_0$ and E_{peak}, for sources that show hybrid spectra in multiple slices.

The value of σ_0 varies significantly within the same GRB.

The evolution trend of σ_0 does not show an obvious relationship with those of lightcurve and E_{peak}.

5. Summary

In this work, we conducted an extensive analysis of the time-resolved spectrum for all Fermi GRBs with known redshift, and we diagnose σ_0 for each time bin by contrasting the thermal and nonthermal radiation components. Our results suggest that:

Most GRB jets should contain a significant magnetic energy component, likely with magnetization factors $\sigma_0 \geq 10$. In this case, the prompt emission mainly arises from magnetized dissipation in such highly magnetized environments as particle acceleration via internal shocks is suppressed.

The value of σ_0 seems vary significantly within the same GRB. And the evolution trend of σ_0 does not show an obvious relationship with those of lightcurve and E_{peak}.

Thanks